

Thermodynamics of the Binding of the C-Terminal Repeat Domain of *Streptococcus sobrinus* Glucosyltransferase-I to Dextran[†]

Hideyuki Komatsu,^{*,‡} Motoki Katayama,[‡] Masaki Sawada,[‡] Yukie Hirata,[‡] Miyuki Mori,[‡] Tetsuyoshi Inoue,[§] Kazuhiro Fukui,[§] Harumi Fukada,^{||} and Takao Kodama[‡]

Department of Bioscience and Bioinformatics, Kyushu Institute of Technology, Iizuka 820-8502, Japan, Department of Oral Microbiology, Okayama University Graduate School of Medicine, Dentistry, and Pharmaceutical Science, Okayama 700-8525, Japan, and Division of Applied Biological Sciences, Graduate School of Life and Environmental Sciences, Osaka Prefecture University, Sakai 599-8531, Japan

Received February 9, 2007; Revised Manuscript Received April 19, 2007

ABSTRACT: Glucosyltransferases (GTFs) secreted by mutans streptococci and some other lactic acid bacteria catalyze glucan synthesis from sucrose, and possess a C-terminal glucan-binding domain (GBD) containing homologous, directly repeating units. We prepared a series of C-terminal truncated forms of the GBD of *Streptococcus sobrinus* GTF-I and studied their binding to dextran by isothermal titration calorimetry. The binding of all truncates was strongly exothermic. Their titration curves were analyzed assuming that the GBD recognizes and binds to a stretch of dextran chain, not to a whole dextran molecule. Both the number of glucose units constituting the dextran stretch (n) and the accompanying enthalpy change (ΔH°) are proportional to the molecular mass of the GBD truncate, with which the Gibbs energy change calculated by the relation $\Delta G^\circ = -RT \ln K$ (R , the gas constant; T , the absolute temperature; K , the binding constant of a truncate for a dextran stretch of n glucose units) also increases linearly. For the full-length GBD (508 amino acid residues), $n = 33.9$, $K = 4.88 \times 10^7 \text{ M}^{-1}$, and $\Delta H^\circ = -289 \text{ kJ mol}^{-1}$ at 25 °C. These results suggest that identical, independent glucose-binding subsites, each comprising 14 amino acid residues on average, are arranged consecutively from the GBD N-terminus. Thus, the GBD binds tightly to a stretch of dextran chain through the adding up of individually weak subsite/glucose interactions. Furthermore, the entropy change accompanying the GBD/dextran interaction as given by the relation $\Delta S^\circ = (\Delta G^\circ - \Delta H^\circ)/T$ has a very large negative value, probably because of a loss of the conformational freedom of dextran and GBD after binding.

Glucosyltransferases (GTFs)¹ or glucansucrases (EC 2.4.1.5) are extracellular enzymes produced by several groups of lactic acid bacteria, including mutans streptococci. They catalyze the transfer of glucosyl units derived from the cleavage of sucrose to a growing α -glucan chain (1). One of several characteristic properties of these enzymes is their high affinity for α -glucans produced by their own actions. Hence, GTFs are conventionally grouped as glucan-binding proteins (GBPs: reviewed in ref 2). With one known exception (3), the glucan-binding domain (GBD) is located in the C-terminal portion of GTFs containing approximately 500 amino acids (4).

The GBD is composed of a series of homologous tandem repeats. Based on the degree of sequence similarity, these repeats have been grouped into four different classes, namely, A, B, C, and D repeats, although all the repeats are immunologically cross-reactive (5). These repeats vary in length from 20 to 48 amino acid residues, but all of them include highly conserved glycine and aromatic residues. The A-repeat motif is universally found in the GBDs of all GTFs and in nonenzyme GBPs of mutans streptococci (1, 2). It has sequence similarity to the cell wall (CW)-binding motifs of toxins A and B of *Clostridium difficile* and the lysins of *Streptococcus pneumoniae* (6, 7). However, it has recently been shown that proteins containing the A-repeat motif and those containing the CW-binding motif have different binding specificities to carbohydrate ligands (8). A hypothesis was also proposed to explain the similarity/dissimilarity in the sequence and size of these repeats, which suggests that repeat sequences evolve from multiple duplication of a common fundamental repeat ("YG" motif) in response to selective pressure (9).

With regard to the role of GBD repeats, a number of studies have been performed to understand the importance of some specific amino acid residues in such repeats for glucan binding as well as the minimum number of repeats essential for GTF functions (8, 10–13). Dissociation con-

[†] This work was supported in part by Grant-in-Aid for Scientific Research (B) 13557161 and (C) 13671904 (to K.F.) and (C) 13680744 (to T.K.) and for Young Scientists (B) 13080537 (to H.K.) from the Ministry of Education, Culture, Sports, Science, and Technology of Japan.

* Corresponding author. Tel: 81-948-29-7845. Fax: 81-948-29-7801. E-mail: hide@bio.kyutech.ac.jp.

[‡] Kyushu Institute of Technology.

[§] Okayama University Graduate School of Medicine, Dentistry, and Pharmaceutical Science.

^{||} Osaka Prefecture University.

¹ Abbreviations: GTF, glucosyltransferase; GBD, glucan-binding domain; GBP, glucan-binding protein; GdnHCl, guanidine hydrochloride; MOPS, 3-(*N*-morpholino)propanesulfonic acid; ITC, isothermal titration calorimetry; DSC, differential scanning calorimetry, CD, circular dichroism.

stants have recently been estimated for the binding of the GBDs of GTFs and GBPs to dextran (8, 14). Although these studies have revealed the structural and functional significance of the repeat structure of GBDs, the mechanism of their interaction with glucans is poorly understood. For example, it has not yet been elucidated whether a GBP molecule recognizes and binds to a whole glucan molecule or a stretch of its chain. In other words, the stoichiometric relationship between the GBD and glucan remains to be determined. It is also unknown what kinds of interactive forces are effective between GBP and glucan.

In this study, we prepared a series of genetically truncated forms of a catalytic domain-deficient GBD from *Streptococcus sobrinus* 6715 (serotype g) GTF-I (15, 16), which consists of six A repeats and five C repeats, and analyzed the interaction of these forms with dextran by isothermal titration calorimetry (ITC). The catalytic domain-deficient GBDs exhibit significant glucan binding and are useful to analyze the binding characteristics (8, 9, 13–15). Dextran is a glucan that is composed of contiguous α -1,6-linked D-glucopyranose units containing a small percentage of mostly α -1,3-linked branching points and is routinely used in most experimental studies on GTFs and GBPs. The ITC data was analyzed assuming that the GBD recognizes and binds to a dextran stretch consisting of a certain number of glucose units. We thus estimated its number together with accompanying thermodynamic parameters (Gibbs energy change and enthalpy and entropy changes). These parameters thus estimated are linear functions of the number of amino acid residues constituting the GBD truncates. The implications of this result together with the nature of GBD/dextran interaction (sources of enthalpy and entropy changes) are discussed in the light of the structural characteristics of both the GBD and dextran.

EXPERIMENTAL PROCEDURES

Chemicals. Dextran T25 (dextran standard 25,000; $M_w/M_n = 1.3$) and T10 (10 kDa; $M_w/M_n = 1.7$) were purchased from Fluka and Pharmacia, respectively. Other chemicals were of analytical grade.

Plasmid Construction. Plasmids of pGBD6R that encodes the full-length GBD (amino acids 1084–1592) from *S. sobrinus* GTF-I and pGBD4RS that encodes a fragment containing four N-terminal A repeats (amino acids 1084–1329) were constructed by inserting the *Hind*III-digested segments of pAB5 and pAB2 (15), respectively, at the *Hind*III site in the multicloning site of pUC18. Other plasmids encoding the GBD truncates with different lengths (pGBD2R, pGBD3R, pGBD4RL, and pGBD5R) were prepared by introducing a stop codon into pGBD6R at the start of each A repeat (Figure 1). The QuikChange Site-Directed Mutagenesis Kit (STRATAGENE) was used for site-directed mutagenesis. All plasmids encoded a cysteine-containing extra peptide (TMITNSSSVPGDPLESTCRH) from pUC18 at the N-terminal end of the GBD truncate (see below).

Protein Expression and Preparation. Proteins were extracted from *Escherichia coli* JM109 transformed with the constructed plasmids and grown at 37 °C in 2 \times YT medium containing 100 μ g mL⁻¹ ampicillin (15). The protein expression was induced by isopropyl- β -D-thiogalactoside at an OD_{660nm} of 1.0. After 3 h of incubation, the cells were

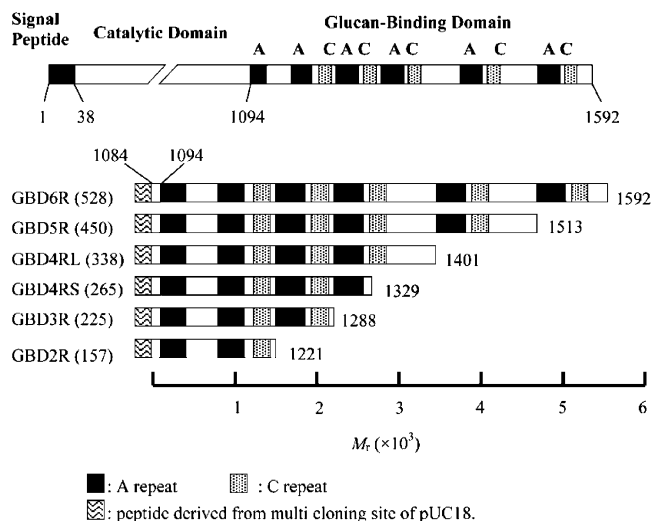


FIGURE 1: Schematic structures of GBD-truncated proteins. GBD truncates start at Ile1084 of GTF-I and terminate at the amino acid numbers indicated on the right; the truncates are named based on the number of A repeats (black bars). The figures in parentheses indicate the number of amino acid residues in GBD truncates.

harvested by centrifugation and washed twice with 5 mM MgCl₂, 5 mM KCl, and 10 mM Tris-HCl (pH 7.4). The cells were stored in a freezer (–20 °C) until use. Frozen cells were suspended in 4 M guanidine hydrochloride (GdnHCl)/10 mM K-phosphate buffer (pH 6.8) and treated by an ultrasonic disruptor (UD-201; Tomy Seiko Co., Tokyo, Japan) for 5 min on ice. The suspension was centrifuged, and the supernatant was dialyzed against 10 mM K-phosphate buffer (pH 6.8) for GBD2R, GBD4RS, GBD4RL, and GBD5R; against the same buffer supplemented with 1.5 M GdnHCl and 1 M NaCl for GBD3R; and against the same buffer supplemented with 0.2 M GdnHCl and 1 M NaCl for GBD6R. After removing the insoluble material by centrifugation, the extract was mixed with Sephacryl S-300 (Pharmacia) equilibrated with 10 mM K-phosphate buffer (pH 6.8). The gel was washed with the same buffer and poured into a column (12 \times 280 mm). The adsorbed proteins were eluted by a linear 0–4 M GdnHCl gradient in 10 mM K-phosphate buffer (pH 6.8) (17). GBD2R and GBD3R were eluted at GdnHCl concentrations of 1.5 and 2.6 M, respectively, and the other GBD proteins at 3.2 M. The main eluted peak contained the monomers and dimers of the expressed GBD proteins. The dimer was formed by disulfide cross-linking via the cysteine residue in the N-terminal extra peptide, as described above. Hence, the sample was first treated with 10 mM dithiothreitol at 25 °C for 30 min and dialyzed against 10 mM K-phosphate buffer (pH 6.8) for 3 h, and the cysteine residue was then alkylated with 10 mM *N*-ethylmaleimide at 25 °C for 30 min. The protein was again adsorbed onto Sephacryl S-300 and eluted with 4 M GdnHCl/10 mM K-phosphate buffer (pH 6.8). The purity of protein samples was examined by SDS–PAGE (Figure 2).

Protein and Dextran Concentrations. Protein concentration was determined from the absorbance at 280 nm using a molar extinction coefficient, which was calculated from the deduced amino acid compositions (15, 18). Dextran concentration was determined by the phenol–sulfuric acid method by using glucose as the standard (19).

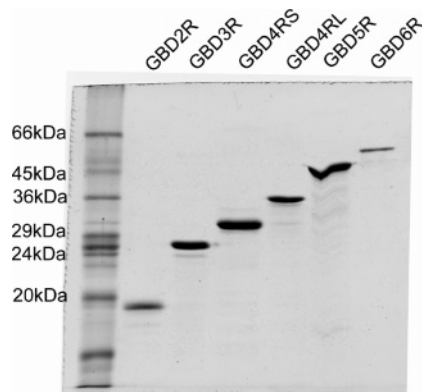
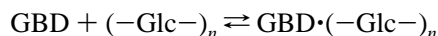


FIGURE 2: SDS-PAGE of purified GBD truncates. The far left lane is a mixture of molecular weight markers.

Isothermal Titration Calorimetry. An MCS-ITC (MicroCal, Inc.) was used at 5 °C, 15 °C, and 25 °C. Protein samples were dialyzed against 10 mM K-phosphate (pH 6.8) or the same buffer supplemented with 0.2 M GdnHCl and 1 M NaCl to increase the solubility of truncated GBDs. Dextran (T10 or T25) was dissolved in the same buffer as that used for dialysis, and an aliquot of the solution was injected every 5 min into the protein solution until no further heat production was observed. The dextran concentrations used were as follows: 0.9–2.5 mg mL⁻¹ for GBD4RS, GBD4RL, and GBD5R and 0.18–0.3 mg mL⁻¹ for GBD6R. The protein concentrations used were as follows: GBD4RS, 14.7–16.8 μM; GBD4RL, 12.0–12.5 μM; GBD5R, 11.8–12.1 μM; and GBD6R, 0.90–2.25 μM. For all experiments, the heat of mixing was measured by injecting the dextran solution into the dialysis buffer.

Data Analysis. We assumed that one molecule of GBD binds to a stretch of dextran chain consisting of n glucose units, $(-Glc-)_n$, forming the complex, $GBD \cdot (-Glc-)_n$:



The equation for fitting binding isotherms for this interaction can be derived as follows. First, the concentration of dextran is converted into its glucose equivalent concentration ($[Glc]_t$), which gives the total concentration of the dextran stretch as $[Glc]_t/n$. The equilibrium (binding) constant (K) for GBD binding to a dextran stretch is then related to the total GBD concentration ($[GBD]_t$) as follows:

$$K = \frac{[GBD]_t Y}{[GBD]_t (1 - Y) \frac{[Glc]_t}{n}} = \frac{Y}{(1 - Y) \frac{[Glc]_t}{n}} \quad (1)$$

$$\frac{[Glc]_t}{n} = \frac{[Glc]_t}{n} + Y[GBD]_t \quad (2)$$

where Y is the fraction of the dextran stretch-bound form of GBD and $[Glc]_t/n$ is the free dextran stretch concentration; hence $[GBD]_t Y$ and $[GBD]_t (1 - Y)$ are concentrations of dextran stretch-bound and free GBD, respectively. Combining eqs 1 and 2 gives the quadratic equation for Y , which is solved as follows:

$$Y = \frac{1}{2} \times \left\{ 1 + \frac{1}{K[GBD]_t} + \frac{[Glc]_t}{n[GBD]_t} - \sqrt{\left(1 + \frac{1}{K[GBD]_t} + \frac{[Glc]_t}{n[GBD]_t} \right)^2 - 4 \times \frac{[Glc]_t}{n[GBD]_t}} \right\} \quad (3)$$

The observed heat q should be proportional to the amount of the dextran stretch-bound GBD in the volume of the reaction cell (V_0 , 1.3 mL), which is hence related to the enthalpy change per mole of the GBD (ΔH) as follows:

$$q = Y[GBD]_t V_0 (-\Delta H) \quad (4)$$

The raw ITC data were integrated and corrected for the mixing heat of dextran using the software (the Origin Lab) installed in the MCS-ITC instrument. To obtain the binding parameters for the model described above, the cumulative heat was plotted as a function of the molar ratio of the glucose equivalent concentration of dextran to the protein concentration. The titration curve thus obtained was fitted to eq 4 by using the analytically determined values of $[GBD]_t$ and $[Glc]_t$ with K , ΔH , and n as adjustable parameters, for which “the user-defined function tool” in the data analysis program of the Origin software (ver. 6.1J) was used.

The thermodynamic parameters are all given as the GBD-mole based values unless otherwise specified. The standard Gibbs energy change ΔG° and the standard entropy change ΔS° were calculated using the equations $\Delta G^\circ = -RT \ln K$ and $\Delta G^\circ = \Delta H^\circ - T\Delta S^\circ$, respectively, where R is the gas constant and T is the absolute temperature. The standard enthalpy change ΔH° is routinely approximated by the observed enthalpy change.

Circular Dichroism. A JASCO J-720 spectropolarimeter was used to record the circular dichroism (CD) spectra of the GBD (11.8 μM GBD4RS, 4.7 μM GBD4RL, 6.6 μM GBD5R, and 1.0 μM GBD6R) in 10 mM K-phosphate buffer (pH 6.8) at 20 °C using a quartz cell with a path length of 1 mm. The spectra were measured from 200 to 250 nm.

Differential Scanning Calorimetry. The heat capacity of truncated GBDs (0.1–0.3 mg mL⁻¹ in 10 mM K-phosphate buffer (pH 6.8) containing 0.2 M GdnHCl and 1 M NaCl) was measured in a VP-DSC (MicroCal, Inc.). Temperature was scanned at a rate of 1 °C min⁻¹. The enthalpies of unfolding were evaluated from the area between the differential scanning calorimetry (DSC) trace and the baseline that is linearly interpolated between pre- and post-transition baselines.

RESULTS

Preparation of GBD Truncates. A series of the truncated forms of the GBD from *S. sobrinus* GTF-I were prepared in a manner such that each truncate contained different numbers of A or C repeats (Figure 1). All the truncated forms were found to bind to Sephacryl (cross-linked dextran gels); hence they were purified by repeated adsorption onto Sephacryl gel followed by elution with GdnHCl (Figure 2). The recovery rates after the second adsorption/elution step were 70%–90%. This indicates that their denaturation by GdnHCl is reversible. The method using α-1,6-glucan-containing matrices and GdnHCl was earlier employed for purifying GTF from *S. sobrinus* (17).

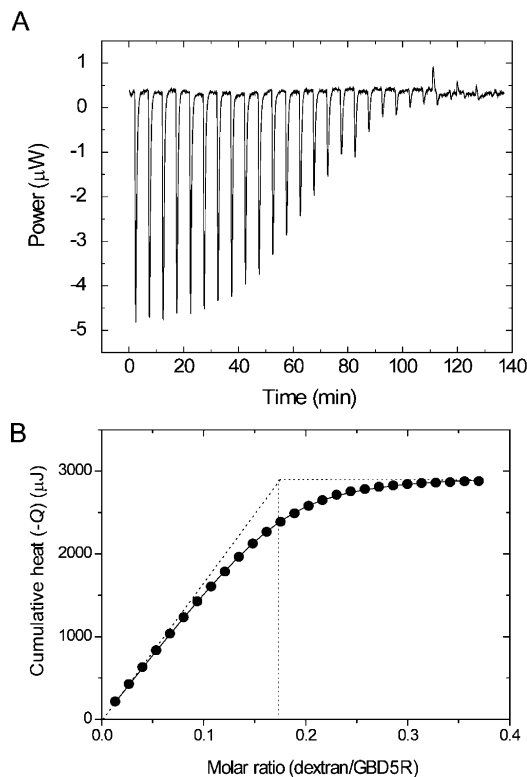


FIGURE 3: The calorimetric titration of a GBD truncate with dextran. (A) A representative thermogram. ITC was performed by injecting $3\ \mu\text{L}$ of dextran T25 solution ($1.8\ \text{mg mL}^{-1}$) into $1.3\ \text{mL}$ (initial volume) of $11.8\ \mu\text{M}$ GBD5R at 5 min intervals. (B) A representative binding isotherm. The cumulative heat (Q) was corrected for the heat of mixing of dextran with buffer and the values of $-Q$ were plotted as a function of the molar ratio of dextran T25 to GBD. The data are fitted using a nonlinear least-squares method with an assumption of 1:1 binding between dextran T25 and GBD molecules. The values of n , K , and ΔH are 0.18, $1.2 \times 10^7\ \text{M}^{-1}$, and $-186\ \text{kJ mol}^{-1}$, respectively. The intersection of the initial slope of the increase in cumulative heat with the line denoting the maximum value of the heat gives the inflection point (dotted lines).

The solubility of the GBD truncates was not high, ranging from 5 to $20\ \mu\text{M}$ in low salt buffers such as $10\ \text{mM}$ K-phosphate buffer (pH 6.8). Therefore the supplementation of GdnHCl ($0.2\ \text{M}$) and NaCl ($1\ \text{M}$) was essential to increase the solubility of the GBD truncates for ITC. As indicated by the finding that the GBD truncates did not dissociate from the Sephacryl gel at GdnHCl concentrations below $1\ \text{M}$ (see Experimental Procedures), the addition of GdnHCl at concentrations up to $0.2\ \text{M}$ hardly affects the binding of the GBD truncates to dextran. In addition, the far-UV CD spectrum of GBD4RS obtained in the presence of $0.2\ \text{M}$ GdnHCl and $1\ \text{M}$ NaCl was not significantly different from that in their absence (See Figure S1 of the Supporting Information).

ITC of Dextran Binding to GBD Truncates. ITC using dextran as the titrant was performed for a series of GBD truncates, except for GBD3R and GBD2R (their affinity for dextran was too low to be measured using the ITC instrument). A representative result (dextran T25 vs GBD5R) is shown in Figure 3. The exothermic heat signal was observed following each injection of dextran into the GBD solution (Figure 3A).

The ITC data were initially analyzed assuming that a GBD molecule binds to a whole dextran molecule; hence the

cumulative heat was plotted as a function of the molar ratio of T25 to GBD5R (Figure 3B). While the plot shows that the dextran has saturable binding to GBD with no characteristic feature of cooperative binding, it also suggests that the binding stoichiometry between dextran and GBD as indicated by the inflection point is unusually low. The curve-fitting analysis indicated that the value of binding stoichiometry was as low as 0.18, which decreased further to 0.12 for GBD4RS (data not shown). Since it was highly unlikely that such a large fraction of the protein could not bind to dextran due to denaturation (if this were the case, the ΔH° for undenatured GBD would be unrealistically large), these results suggested a novel view of the GBD/dextran interaction. Thus, several molecules of GBD can bind to a single chain of dextran. In other words, the GBD may be a protein that recognizes and binds to a stretch of dextran chain rather than a whole dextran molecule. In addition, the length of such a stretch itself may vary with the molecular size of the GBD truncate.

ITC data for a series of GBD truncates were then analyzed to determine the length of a stretch of dextran chain interacting with the truncate as well as other binding parameters. For this purpose, dextran concentrations were converted into glucose equivalent concentrations, and the observed heat was plotted as a function of their molar ratio to the protein for all GBD truncates examined at three different temperatures (Figure 4). The heat at saturating concentrations of dextran, corresponding to the enthalpy change ΔH° for dextran binding of a GBD truncate, increased with the molecular mass of truncate. As can be seen intuitively, the molar ratio at which the inflection point of the isotherm occurs also increased in a similar manner. Analysis was then carried out using a simplifying model assuming that the GBD binds to a stretch of dextran chain consisting of a certain number of glucose units. The titration curves were fitted to obtain the ITC parameters, and the calculated thermodynamic parameters are summarized in Table 1.

Table 1 also shows the data regarding the effects of high salt concentration ($0.2\ \text{M}$ GdnHCl + $1\ \text{M}$ NaCl), dextran size (T10 vs T25), and buffer component (phosphate vs 3-(*N*-morpholino)propanesulfonic acid (MOPS)). It is apparent that these variations in the ITC conditions did not significantly affect the binding parameters and the inferred thermodynamics of GBD binding to dextran. However, the n and ΔH° values observed in the absence of $0.2\ \text{M}$ GdnHCl and $1\ \text{M}$ NaCl were slightly smaller than those observed in their presence. This may result from a slight protein aggregation caused by the low solubility of the GBD truncates. It was noted that the ΔH° value measured in phosphate buffer was not very different from that measured in MOPS buffer. This suggests that the protonation heat of the buffer (ΔH_{buffer}) does not contribute to the observed enthalpy; this is because the ΔH_{buffer} values for phosphate and MOPS are 5.1 and $21.8\ \text{kJ mol}^{-1}$, respectively (20). In other words, no net proton exchange occurs upon the binding of GBDs to dextran.

Thermodynamic Parameters for the Binding of GBD Truncates to Dextran. The negative ΔH° value, the number of glucosyl units interacting with the GBD truncate (n), and the binding constant (K) increased with the size of the truncate. However, while ΔH° and K values showed small

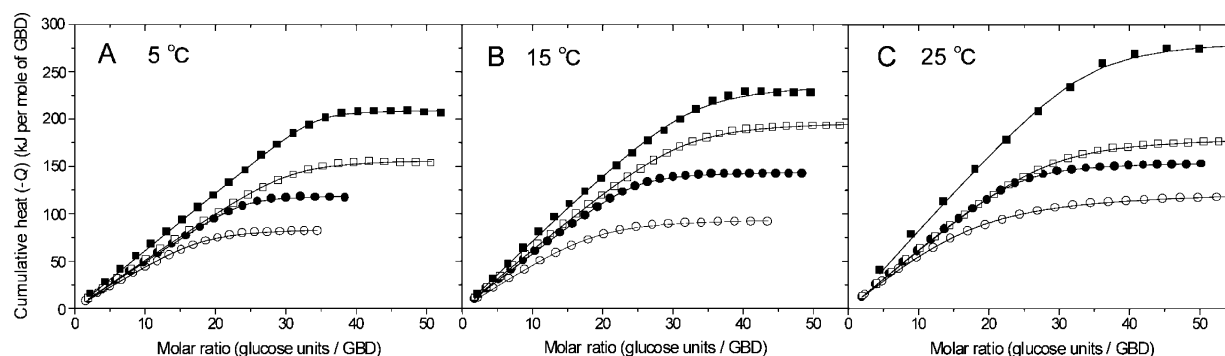


FIGURE 4: Plots of the binding heat as a function of the molar ratio of glucose units of dextran to GBD. The cumulative heats ($-Q$) were converted into heat per mole of the GBD truncates. Panels A, B, and C show data obtained at 5 °C, 15 °C, and 25 °C, respectively. Open circles, closed circles, open squares, and closed squares indicate the heat of GBD4RS, GBD4RL, GBD5R, and GBD6R, respectively. The titration curves were fitted to eq 4 with parameters from Table 1 (solid lines).

Table 1: Thermodynamic Parameters of the Binding of Truncated GBDs to Dextran^a

protein	$T(^{\circ}\text{C})$	ITC parameters			calculated parameters ^b		
		ΔH° (kJ mol ⁻¹)	n	K (M ⁻¹)	ΔG° (kJ mol ⁻¹)	ΔS° (kJ K ⁻¹ mol ⁻¹)	ΔC_p^c (kJ K ⁻¹ mol ⁻¹)
GBD4RS	5.0	-86.5	18.3	1.92×10^6	-33	-0.19	-2.0 ± 0.3
	15.0	-101	19.3	1.18×10^6	-33	-0.23	
	25.0	-127	18.0	3.96×10^5	-32	-0.32	
	25.0 ^d	-109	15.8	4.50×10^5	-32	-0.26	
	25.0 ^e	-136	18.0	2.29×10^5	-31	-0.35	
	25.0 ^f	-137	17.8	6.08×10^5	-33	-0.35	
GBD4RL	5.0	-121	24.0	9.86×10^6	-37	-0.30	-1.7 ± 0.5
	15.0	-146	24.5	6.47×10^6	-38	-0.38	
	25.0	-155	24.4	3.05×10^6	-37	-0.40	
GBD5R	5.0	-160	30.8	6.16×10^6	-36	-0.45	-1.2 ± 1.7
	15.0	-201	31.8	3.50×10^6	-36	-0.57	
	25.0	-184	28.0	2.31×10^6	-36	-0.50	
GBD6R	5.0	-214	34.2	1.34×10^8	-43	-0.61	-3.8 ± 1.0
	15.0	-234	33.3	2.90×10^7	-41	-0.67	
	25.0	-289	33.9	4.88×10^7	-44	-0.82	

^a All measurements were carried out using dextran T25 in 10 mM K-phosphate buffer (pH 6.8) containing 0.2 M GdnHCl and 1 M NaCl unless otherwise indicated. The fitting errors of ITC parameters were in the range of 6.0–20 kJ mol⁻¹ for ΔH° and 1.0–2.0 for n , whereas the corresponding values for the binding constant (K) were well within a half order of magnitude or equivalent to a range of ± 2 kJ mol⁻¹ for ΔG° . ^b $\Delta G^{\circ} = -RT \ln K$; and $\Delta S^{\circ} = (\Delta G^{\circ} - \Delta H^{\circ})/T$. ^c The slope of the regression line with the fitting error of the ΔH° plot versus temperature. ^d Measured in 10 mM K-phosphate buffer (pH 6.8) not containing 0.2 M GdnHCl and 1 M NaCl. ^e Dextran T10 was used. ^f Measured in 10 mM MOPS buffer (pH 6.8) containing 0.2 M GdnHCl and 1 M NaCl.

but clear temperature dependence, the n values were independent of temperature.

The binding constant between a GBD truncate and a dextran stretch ranges from 10^6 to 10^8 M⁻¹, the inverse values of which are in reasonable agreement with the dissociation constants previously estimated by different methods for the dextran binding of the GBD of GTFs and GBPs (8, 14). For all truncates, the ΔG° value ($= -RT \ln K$) was less negative than the ΔH° value; therefore, dextran binding is accompanied by a large negative ΔS° ($= (\Delta H^{\circ} - \Delta G^{\circ})/T$).

Thermodynamic Dissection of the GBD into Binding Subsites. All the binding parameters vary with the molecular mass of the GBD truncate; hence, we plotted the thermodynamic parameters as a function of the number of residues counted from the N-terminus of the GBD (Figure 5). The value of n is proportional to the number of amino acid residues (Figure 5A). This result strongly indicates that the GBD consists of multiple, identical, independent glucose-binding sites, each of which interacts with a glucose unit on a single dextran chain. The slope of the regression line is equal to 0.070 with the unit of glucose units per amino acid residue of GBD. Taking its reciprocal, a round value of 14 was obtained. Since its unit is then the number of residues

per glucose unit, it is the average number of amino acid residues that constitute a GBD subsite interacting with a glucose unit of a dextran stretch recognized by a whole GBD.

The $-\Delta H^{\circ}$ value is also proportional to the number of amino acid residues (Figure 5B, closed symbols), with which the $-\Delta G^{\circ}$ varies linearly as well though not markedly (Figure 5B, open symbols). These facts substantiate that all glucose-binding subsites are identical and independent. The enthalpy change for the glucose-binding subsite to interact with a glucose unit ($-\Delta H^{\circ}/n$) can be estimated as 6–9 kJ mol⁻¹ at 25 °C. Since the $-\Delta G^{\circ}$ marginally depends on the number of amino acid residues, the $-T\Delta S^{\circ}$ ($= \Delta G^{\circ} - \Delta H^{\circ}$) linearly increases just like the $-\Delta H^{\circ}$ (Figure 5C).

Conformation and Thermal Stability of the GBD Truncates. The decrease in the binding affinity of the GBD truncates that are shorter than GBD6R might be caused by improper conformation and/or instability of the proteins. Therefore, we tested whether the deletion of C-terminal residues significantly altered the conformation and stability of GBD truncates (GBD4RS, GBD4RL, GBD5R, and GBD6R). First, the conformations of GBD truncates were analyzed by far-UV CD. All CD spectra showed a broad maximum at 227 nm (Figure 6), which is consistent with

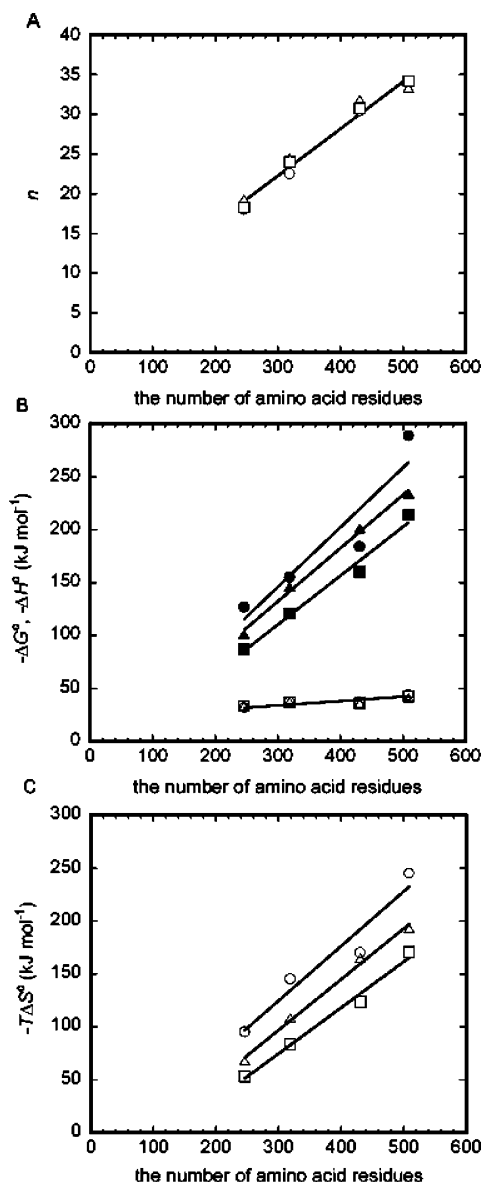


FIGURE 5: Thermodynamic parameters as a function of the number of amino acid residues in GBD truncates. (A) Number of glucose units interacting with GBD truncates, n . (B) Binding Gibbs energy change, $-\Delta G^\circ$ (open symbols), and binding enthalpy, $-\Delta H^\circ$ (closed symbols). (C) Binding entropy term, $-T\Delta S^\circ$. Data obtained at 5 °C, 15 °C, and 25 °C shown as squares, triangles, and circles, respectively, were plotted against the number of amino acid residues corrected for the 20 extra residues translated from the vector pUC18. For $-\Delta H^\circ$ and $-T\Delta S^\circ$, a linear regression line was fitted to a data set obtained at different temperatures, while the regression lines for n and $-\Delta G^\circ$ were fitted by ignoring the temperature effect.

high β -sheet and random coil contents in the GBD secondary structure predicted from the amino acid sequence of the GBD portion of *S. sobrinus* GTF-I (15). This result also shows a good agreement with that reported earlier for GBP-A (21) and the GBD of GTF-J (13). Next, the thermal stability of the GBD truncates was examined by DSC. Each protein shows an endothermic unfolding transition with T_m around 40 °C, which slightly shifts toward higher temperatures with an increase in the truncate size (Figure 7). Furthermore, in all the GBD truncates measured, the values of the weight-based specific calorimetric enthalpy for their thermal transition fall within a range of values generally observed for compact proteins (22–30 kJ g⁻¹) (22). These results indicate

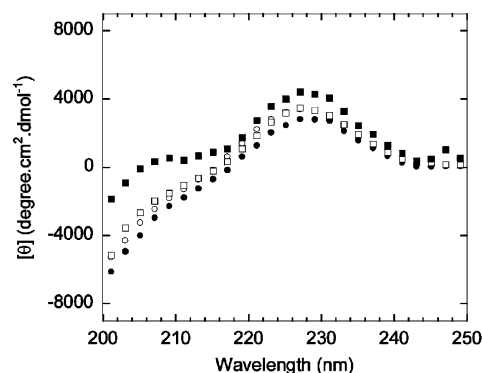


FIGURE 6: Circular dichroism spectra of GBD4RS (open circles), GBD4RL (closed circles), GBD5R (open squares), and GBD6R (closed squares) in 10 mM K-phosphate buffer (pH 6.8) at 20 °C.

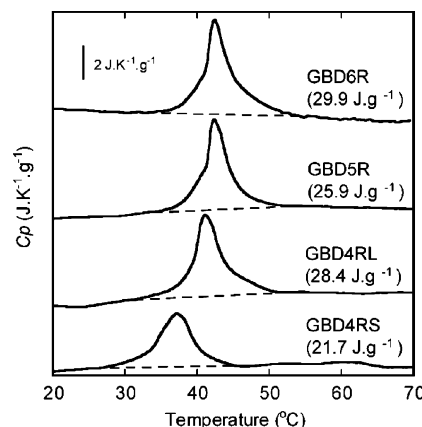


FIGURE 7: Thermal unfolding of GBD truncates in 10 mM K-phosphate buffer (pH 6.8) containing 0.2 M GdnHCl and 1 M NaCl. Pre- and post-transition baselines are connected linearly (dashed lines). The peaks of the C_p of GBD4RS, GBD4RL, GBD5R, and GBD6R are 37.2 °C, 41.1 °C, 42.4 °C, and 42.5 °C, respectively. The numbers in parentheses indicate the weight-based specific calorimetric enthalpies, which were estimated from the area under the peak of each DSC trace.

that, regardless of molecular mass, the secondary structures and thermal stability are similar in all the GBD truncates tested. Therefore, the deletion of C-terminal residues does not greatly alter the conformation and stability of the GBD truncate (GBD4RS to GBD6R). This result is also consistent with the fact that the GBD is composed of many identical structural units.

DISCUSSION

Binding of Dextran as a Multivalent Ligand to the GBD Repeat Domain. In earlier studies on interaction of GBPs with dextran, it appears that the molar binding stoichiometry of 1:1 has been tacitly assumed between protein and glucan molecules. In this study, however, we showed that the GBD recognizes and binds to a stretch of α -1,6-linked chain rather than a whole dextran molecule. Our basic assumption is that dextran is a linear array of ligands (glucose units). A similar assumption was first used when analyzing the interaction of basic fibroblast growth factor with heparin (23), a polysaccharide chain containing repeating disaccharide units composed of D-glucosamine and uronic acid. However, the GBD/dextran binding is unique in that it is an interaction between a protein having multiple ligand-binding sites and dextran as a homo-polydentate carbohydrate ligand.

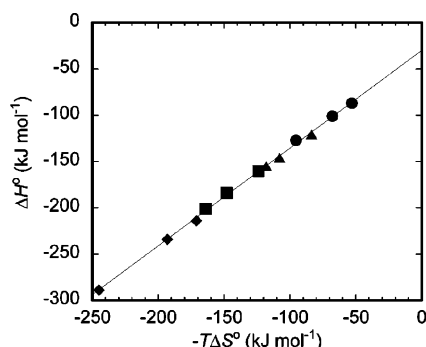


FIGURE 8: Plot of ΔH° as a function of $-T\Delta S^\circ$. Circles, triangles, squares, and diamonds represent the parameters for GBD4RS, GBD4RL, GBD5R, and GBD6R, respectively. A straight line was drawn by linear regression for pooled data of all truncates.

Based on the proportionality of the thermodynamic parameters to the number of residues in the GBD, GBD can be dissected into the glucose-binding subsites consisting of 14 amino acid residues on average. A tacit assumption is that the subsites are arranged throughout the entire GBD sequence regardless of their structures. By contrast, in earlier proposals, GBD repeats have been classified based on sequence analysis data and defined to have lengths ranging between 14 and 48 residues (8, 24, 25). A characteristic feature common to these repeats is that all include conserved glycine and aromatic residues (tryptophan, tyrosine, and phenylalanine). The importance of these residues has recently been demonstrated by site-directed mutagenesis (8). Among these repeats, the YG repeat is of interest in the present context because it consists of 21 residues, and as many as 23 of its homologues are almost evenly distributed in the GBD used in this study (26). Thus, according to the present result, two YG repeats ($21 \times 2 = 42$ residues) may correspond to three of the aforementioned glucose-binding units together ($14 \times 3 = 42$ residues). In other words, a plausible hypothesis is that two YG repeats fold into a tertiary structure so that the conserved aromatic residues interact with three glucose units. It was proposed that the repeats classified by a different criterion (A, B, C, and D) have evolved from multiple duplication of an ancestral homologue of the YG repeat (9). If this were the case, one or more glucose-binding units would also be included in these sequence-based repeats. For example, the highly conserved A repeat consisting of 33 residues (1) can accommodate at least two such units. However, the elucidation of the three-dimensional structure of GBD is prerequisite to reconcile the present thermodynamically defined dissection with the structure-based classification of the GBD repeats.

Thermodynamic Nature of the Interaction between the GBD and Dextran. When plotted against $-T\Delta S$, all ΔH° values lie on the same line irrespective of the truncate sizes (Figure 8). The slope of this line is essentially equal to unity (1.06), indicating that the increase in favorable enthalpy change is almost completely offset by the increase in unfavorable entropy change; this results in a marginal increase in the affinity toward dextran. In other words, all glucose-binding subsites are equivalent in terms of quantitative contribution by enthalpy (energy) and entropy (order) and are arranged in tandem from the GBD N-terminal side. Thus, while each subsite can interact independently but only weakly with a glucose unit, the total effect of a number of

such weak interactions is the molecular basis of the formation of tightly associated dextran–GBD complexes. A similar multivalent interaction has recently been demonstrated by structural and thermodynamic studies on the tight binding between glycogen and pullulanases from *S. pneumoniae* and *S. pyogenes* (27).

Sources of Enthalpy and Entropy Changes. (A) ΔH° . The $-\Delta H^\circ$ values per glucose unit are in the range of 6–9 kJ mol⁻¹. In terms of an interacting monosaccharide unit base, these values are comparable to those of cellulose binding of *Cellulomonas fimi* β -1,4-glucanase C (28). In this case, together with other protein–sugar interactions (29), the observed ΔH° is attributed to the formation of a hydrogen bond between a sugar hydroxyl group and a polar amino acid side chain and/or van der Waals contact between a sugar chain (C–C bonds) and aromatic residues. A number of these amino acid residues occur as major constituents of the repeat structure of GTF-I GBD.

With regard to the temperature dependence of ΔH° , it appears that, for each GBD truncate, the dextran binding is accompanied by a negative value of the heat capacity change (ΔC_p) (Table 1), which is large enough to suggest the release of hydrophobic hydration water (30, 31). However, the accurate estimation of the ΔC_p per glucose unit was hampered in the present study because of the measurements of ΔH° only at three different temperatures and the accompanying experimental errors.

(B) ΔS° . There are three generally accepted major effects in aqueous solution that are accompanied by large entropy changes: changes in solvation (ΔS_{sol}), rotational and translational motions (ΔS_{rt}), and conformations of interacting solutes (ΔS_{conf}) (32). If the release of hydrophobic hydration water is solely responsible for the observed ΔC_p values (Table 1), the corresponding value of ΔS would be very large, approximately 1 kJ K⁻¹ mol⁻¹ for GBD6R at 25 °C (a first approximation using values tabulated for the transfer of hydrocarbons from water to an organic solvent) (33). Although the contribution of the dehydration of dextran to ΔS_{sol} cannot be calculated, we assume that it should be >0 . Thus, a substantial amount of favorable entropy change (ΔS_{sol}) must be offset or rather superseded by an unfavorable entropy decrease from other sources.

According to a recent theory (32), the overall rotational and translational motions contribute negligibly to the binding affinity (free energy) in molecular association/recognition processes in aqueous solutions, i.e., $\Delta S_{\text{rt}} < 10R$. We assume that the rotational and translational entropy is negligible compared with ΔS° .

Thus, a loss of conformational entropy is most likely to be the main component of entropy cost, which probably results from a decrease in the conformational freedom of both dextran and protein upon their binding. We first consider the conformation of dextran by focusing only on its chain entropy. The C5–C6 bond of each glucose unit constituting a dextran chain freely rotates; thus, the chain conformation of dextran closely resembles random coil conformation. A calculation of molecular dynamics revealed six lowest-energy minima at the α -1,6-glucosidic linkage (C1–O1–C6–C5) of isomaltose on the adiabatic map (34). This indicates that 6^{m-1} conformations should exist in an α -1,6-linked polymer of m glucose units. When trapped by GBD-binding sites, the conformational freedom of these units should be greatly

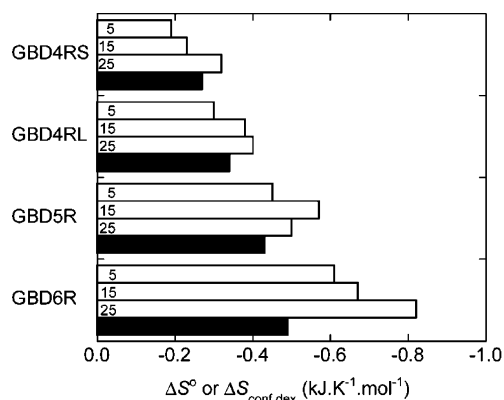


FIGURE 9: Comparison of the observed entropy changes with those calculated from the conformational freedom of the dextran chain. Open and closed bars indicate ΔS° and $\Delta S_{\text{conf,dex}}$, respectively. The figures in the open bar indicate experimental temperatures ($^\circ\text{C}$). Calculations were carried out using the equation $\Delta S_{\text{conf,dex}} = R \ln 6^{n-1}$, where n is the average value of each data set obtained at different temperatures for a given GBD truncate since it is temperature independent (Table 1).

diminished. Quantitatively, the number of conformations of GBD-bound dextran would become negligibly small in comparison to 6^{n-1} . If this were the case, the loss of conformational entropy (chain entropy) of the stretch of dextran chain consisting of n glucose units could be calculated as follows:

$$\Delta S_{\text{conf,dex}} = R \ln 6^{n-1} \quad (5)$$

The values of $\Delta S_{\text{conf,dex}}$ thus calculated are compared with those of the observed ΔS° (Figure 9). Two interesting features are prominent. One feature is that, for a smaller truncate, the calculated dextran entropy loss is roughly equal to the observed entropy decrease. The other feature is that the higher the temperature, the bigger the gap between the calculated and observed values. This might arise in part from the fact that other conformational freedoms of dextran such as intramolecular interaction between branches, which could be temperature dependent, are not considered in the above calculation. Nonetheless, these results suggest that the loss of the conformational freedom of dextran chain must be one of the major sources of entropy cost accompanying the interaction with GBD, and that there exists a protein size- and temperature-dependent source or sources for entropy cost, which are only partly detected by calorimetry.

Thus, another major contribution to entropy cost most likely results from a decrease in the conformational freedom of the GBD protein upon binding to dextran. The secondary structure of the protein with high β -sheet and random coil contents may suggest that the GBD is fairly flexible in structure. In fact, its dextran-induced conformational change is shown by limited proteolysis (35). When a truncated form of GTF-I, which contains the catalytic domain and GBD4RS and exhibits significant dextran binding and glucan synthesis (15, 35), was subjected to tryptic digestion, the GBD portion was rapidly digested in the absence of dextran but not in its presence. This fact supports the notion that the flexibility of the GBD in the unbound state is more or less lost on binding to dextran. Because of the lack of quantitative data, it can only be stated that the magnitude of the conformational change of the GBD should be sufficiently large to offset or

outweigh the undetected favorable entropy gain by dehydration ($\sim 1 \text{ kJ K}^{-1}\text{mol}^{-1}$ for GBD6R).

Comparison with Other Carbohydrate-Binding Proteins. Finally, we should refer to other carbohydrate-binding proteins, e.g., cellulose- and starch-binding proteins (28, 36–39). Their binding to respective ligands is moderately strong ($K > 10^4$ – 10^6 M^{-1}) and is accompanied by negative ΔH° and ΔS° values; therefore, their thermodynamics are qualitatively similar to those of the GBD. However, both ΔH° and ΔS° are significantly smaller, which is probably due to their interaction with considerably smaller sugar units (oligosaccharides consisting of only 3 to 6 sugar units). The important point is that these sugar ligands possess their own structures with more or less constrained geometry and orientation of the chains. The chain conformation freedom is severely limited in the helical α -1,4-linked chain of amylose as well as in the straight β -1,4-linked chain of cellulose, which has been elegantly demonstrated by recent atomic force microscopy (40). This observation is in sharp contrast to the random coil structure of dextran (42). Thus, it appears reasonable that an interaction between the topologically inflexible sugar units and amino acid residues of sugar-binding proteins occurs in a regiospecific manner as shown in the atomic structures of cellulose- and amylose-binding proteins (37, 39, 42). By this virtue, the offsetting effect of unfavorable ΔS would be relatively small. In this regard, the mode of interaction between the random coil/ β -sheet-rich GBD and the flexible dextran chain is remarkably unique. The present study clearly shows that its binding specificity and strength arise from the total sum of individually weak subsite/glucose unit interactions at the cost of a large value of entropy resulting from a loss of the conformational freedom of interacting molecules.

ACKNOWLEDGMENT

We thank Akiyoshi Tanaka of the Faculty of Bioresources, Mie University, for enabling us to perform a DSC analysis of GBD truncates. We appreciate the assistance provided by Aya Kumamaru, Kimiyo Sunagawa, and Kohei Inazumi for plasmid construction, protein preparation, and DSC operation, respectively.

SUPPORTING INFORMATION AVAILABLE

Circular dichroism spectra of GBD4RS in the absence and presence of 0.2 M GdnHCl and 1 M NaCl. This material is available free of charge via the Internet at <http://pubs.acs.org>.

REFERENCES

- Monchois, V., Willemot, R. M., and Monsan, P. (1999) Glucan-sucrose: mechanism of action and structure-function relationships, *FEMS Microbiol. Rev.* 23, 131–151.
- Banas, J. A., and Vickerman, M. M. (2003) Glucan-binding proteins of the oral streptococci, *Crit. Rev. Oral Biol. Med.* 14, 89–99.
- Bozonnet, S., Dols-Laffargue, M., Fabre, E., Pizzut, S., Remaud-Simeon, M., Monsan, P., and Willemot, R. M. (2002) Molecular characterization of DSR-E, an α -1,2 linkage-synthesizing dextransucrase with two catalytic domains, *J. Bacteriol.* 184, 5753–5761.
- Ferretti, J. J., Gilpin, M. L., and Russell, R. R. (1987) Nucleotide sequence of a glucosyltransferase gene from, *Streptococcus sobrinus* MFe28, *J. Bacteriol.* 169, 4271–4278.
- Smith, D. J., Taubman, M. A., Holmberg, C. F., Eastcott, J., King, W. F., and Ali-Salaam, P. (1993) Antigenicity and immunogenicity

- of a synthetic peptide derived from a glucan-binding domain of mutans streptococcal glucosyltransferase, *Infect. Immun.* 61, 2899–2905.
6. Jedrzejewski, M. J. (2001) Pneumococcal Virulence Factors: Structure and Function, *Microbiol. Mol. Biol. Rev.* 65, 187–207.
7. Wren, B. W., Russell, R. R., and Tabaqchali, S. (1991) Antigenic cross-reactivity and functional inhibition by antibodies to *Clostridium difficile* toxin A, *Streptococcus mutans* glucan-binding protein, and a synthetic peptide, *Infect. Immun.* 59, 3151–3155.
8. Shah, D. S., Joucla, G., Remaud-Simeon, M., and Russell, R. R. (2004) Conserved repeat motifs and glucan binding by glucan-sucrases of oral streptococci and *Leuconostoc mesenteroides*, *J. Bacteriol.* 186, 8301–8308.
9. Giffard, P. M., and Jacques, N. A. (1994) Definition of a fundamental repeating unit in streptococcal glucosyltransferase glucan-binding regions and related sequences, *J. Dent. Res.* 73, 1133–1141.
10. Lis, M., Shiroza, T., and Kuramitsu, H. K. (1995) Role of the C-terminal direct repeating units of the *Streptococcus mutans* glucosyltransferase-S in glucan binding, *Appl. Environ. Microbiol.* 61, 2040–2042.
11. Vickerman, M. M., and Clewell, D. B. (1997) Deletion in the carboxyl-terminal region of *Streptococcus gordonii* glucosyltransferase affect cell-associated enzyme activity and sucrose-associated accumulation of growing cells, *Appl. Environ. Microbiol.* 63, 1667–1673.
12. Monchois, V., Reverte, A., Remaud-Simeon, M., Monsan, P., and Willemot, R. M. (1998) Effect of *Leuconostoc mesenteroides* NRRL B-512F dextranucrase carboxy-terminal deletions on dextran and oligosaccharide synthesis, *Appl. Environ. Microbiol.* 64, 1644–1649.
13. Kingston, K. B., Allen, D. M., and Jacques, N. A. (2002) Role of the C-terminal YG repeats of the primer-dependent streptococcal glucosyltransferase, GtfJ, in binding to dextran and mutan, *Microbiology* 148, 549–558.
14. Haas, W., and Banas, J. A. (2000) Ligand-binding properties of the carboxyl-terminal repeat domain of *Streptococcus mutans* glucan-binding protein A, *J. Bacteriol.* 182, 728–733.
15. Abo, H., Matsumura, T., Kodama, T., Ohta, H., Fukui, K., Kato, K., and Kagawa, H. (1991) Peptide sequences for sucrose splitting and glucan binding within *Streptococcus sobrinus* glucosyltransferase (water-insoluble glucan synthetase), *J. Bacteriol.* 173, 989–996.
16. Fukui, K., Moriyama, T., Miyake, Y., Mizutani, K., and Tanaka, O. (1982) Purification and properties of glucosyltransferase responsible for water-insoluble glucan synthesis from *Streptococcus mutans*, *Infect. Immun.* 37, 1–9.
17. Mooser, G., Shur, D., Lyou, M., and Watanabe, C. (1985) Kinetic studies on dextranucrase from the cariogenic oral bacterium *Streptococcus mutans*, *J. Biol. Chem.* 260, 6907–6915.
18. Gill, S. C., and von Hippel, P. H. (1982) Calculation of protein extinction coefficients from amino acid sequence data, *Anal. Biochem.* 182, 319–326.
19. Dubois, M., Gilles, K. A., Hamilton, J. K., Robers, P., and Smith, F. (1956) Colorimetric method for determination of sugars and related substances, *Anal. Chem.* 28, 350–356.
20. Fukada, H., and Takahashi, K. (1998) Enthalpy and heat capacity changes for the proton dissociation of various buffer components in 0.1 M potassium chloride, *Proteins* 33, 159–166.
21. Haas, W., MacColl, R., and Banas, J. A. (1998) Circular dichroism analysis of the glucan binding domain of *Streptococcus mutans* glucan binding protein-A, *Biochim. Biophys. Acta* 1384, 112–120.
22. Pfeil, W. (2001) *Protein Stability and Folding: Collection of Thermodynamic Data*, Springer, Berlin.
23. Arakawa, T., Wen, J., and Philo, J. S. (1994) Stoichiometry of heparin binding to basic fibroblast growth factor, *Arch. Biochem. Biophys.* 308, 276–273.
24. Russell, R. R. (1990) Molecular genetics of glucan metabolism in oral streptococci, *Arch. Oral. Biol.* 35, 53S–58S.
25. Giffard, P. M., Simpson, C. L., Milward, C. P., and Jacques, N. A. (1991) Molecular characterization of a cluster of at least two glucosyltransferase genes in *Streptococcus salivarius* ATCC 25975, *J. Gen. Microbiol.* 137, 2577–2593.
26. Simpson, C. L., Giffard, P. M., and Jacques, N. A. (1995) *Streptococcus salivarius* ATCC 25975 possesses at least two genes coding for primer-independent glucosyltransferases, *Infect. Immun.* 63, 609–621.
27. van Bueren, A. L., Higgins, M., Wang, D., Burke, R. D., and Boraston, A. B. (2007) Identification and structural basis of binding to host lung glycogen by streptococcal virulence factors, *Nat. Struct. Mol. Biol.* 14, 76–84.
28. Tomme, P., Creagh, A. L., Kilburn, D. G., and Haynes, C. A. (1996) Interaction of polysaccharides with the N-terminal cellulose-binding domain of *Cellulomonas fimi* CenC. 1. Binding specificity and calorimetric analysis, *Biochemistry* 35, 13885–13894.
29. Toone, E. J. (1994) Structure and energetics of protein-carbohydrate complexes, *Curr. Opin. Struct. Biol.* 4, 719–728.
30. Privalov, P. L., and Gill, S. J. (1988) Stability of protein structure and hydrophobic interaction, *Adv. Protein Chem.* 39, 191–234.
31. Sturtevant, J. M. (1977) Heat capacity and entropy changes in processes involving proteins, *Proc. Natl. Acad. Sci. U.S.A.* 74, 2236–2240.
32. Yu, Y. B., Privalov, P. L., and Hodges, R. S. (2001) Contribution of translational and rotational motions to molecular association in aqueous solution, *Biophys. J.* 81, 1632–1642.
33. Tanford, C. (1980) *The Hydrophobic effect: Formation of Micelles and Biological Membranes*, 2nd ed., John Wiley and Sons, New York.
34. Best, R. B., Jackson, G. E., and Naidoo, K. J. (2001) Molecular dynamics and NMR study of the $\alpha(1-4)$ and $\alpha(1-6)$ glycosidic linkages: maltose and isomaltose, *J. Phys. Chem. B* 105, 4742–4751.
35. Konishi, N., Torii, Y., Yamamoto, T., Miyagi, A., Ohta, H., Fukui, K., Hanamoto, S., Matsuno, H., Komatsu, H., Kodama, T., and Katayama, E. (1999) Structure and enzymatic properties of genetically truncated forms of the water-insoluble glucan-synthesizing glucosyltransferase from *Streptococcus sobrinus*, *J. Biochem. (Tokyo)* 126, 287–295.
36. Sigurskjold, B. W., Svensson, B., Williamson, G., and Driguez, H. (1994) Thermodynamics of ligand binding to the starch-binding domain of glucoamylase from *Aspergillus niger*, *Eur. J. Biochem.* 225, 133–141.
37. Boraston, A. B., Nurizzo, D., Notenboom, V., Ducros, V., Rose, D. R., Kilburn, D. G., and Davies, G. J. (2002) Differential oligosaccharide recognition by evolutionarily-related β -1,4 and β -1,3 glucan-binding modules, *J. Mol. Biol.* 319, 1143–1156.
38. Arai, T., Araki, R., Tanaka, A., Karita, S., Kimura, T., Sakka, K., and Ohmiya, K. (2003) Characterization of a cellulase containing a family 30 carbohydrate-binding module (CBM) derived from *Clostridium thermocellum* CelJ: importance of the CBM to cellulose hydrolysis, *J. Bacteriol.* 185, 504–512.
39. Boraston, A. B., Healey, M., Klassen, J., Ficko-Blean, E., Lammerts, van Bueren, A., and Law, V. (2006) A structural and functional analysis of α -glucan recognition by family 25 and 26 carbohydrates-binding modules reveals a conserved mode of starch recognition, *J. Biol. Chem.* 281, 587–598.
40. Heymann, B., and Grubmüller, H. (1999) ‘Chair–boat’ transitions and side groups affect the stiffness of polysaccharides, *Chem. Phys. Lett.* 305, 202–208.
41. Rief, M., Oesterhelt, F., Heymann, B., and Gaub, H. E. (1997) Single molecule force spectroscopy on polysaccharides by atomic force microscopy, *Science* 275, 1295–1297.
42. Boraston, A. B., Bolam, D. N., Gilbert, H. J., and Davies, G. J. (2004) Carbohydrate-binding modules: fine-tuning polysaccharide recognition, *Biochem. J.* 382, 769–781.

B1700282C